

Optical Coherence Tomographic Observation of Morphological Features of Neointimal Tissue after Drug-Eluting Stent Implantation

Seung-Yul Lee,¹ Dong-Ho Shin,¹ Jung-Sun Kim,¹ Byeong-Keuk Kim,¹ Young-Guk Ko,¹
Donghoon Choi,¹ Yangsoo Jang,^{1,2} and Myeong-Ki Hong^{1,2}

¹Division of Cardiology, Severance Cardiovascular Hospital, Yonsei University College of Medicine, Seoul;

²Severance Biomedical Science Institute, Yonsei University College of Medicine, Seoul, Korea.

Received: September 3, 2013

Revised: October 23, 2013

Accepted: December 2, 2013

Corresponding author: Dr. Myeong-Ki Hong,

Division of Cardiology,

Severance Cardiovascular Hospital,

Yonsei University College of Medicine,

50-1 Yonsei-ro, Seodaemun-gu,

Seoul 120-752, Korea.

Tel: 82-2-2228-8458, Fax: 82-2-393-2041

E-mail: mkhong61@yuhs.ac

The authors have no financial conflicts of interest.

Purpose: The impacts of different time courses and the degree of neointimal growth on neointimal morphology have not yet been sufficiently investigated. Therefore, we evaluated the morphological features of neointimal tissue after drug-eluting stent (DES) implantation using optical coherence tomography (OCT).

Materials and Methods: The morphological features of neointimal tissue in stented segments with a maximal percentage of cross-sectional area (CSA) stenosis of neointima were evaluated in 507 DES-treated lesions with >100 μ m mean neointimal thickness on follow-up OCT. Neointimal tissue was categorized as homogeneous, heterogeneous, layered, or neoatherosclerotic. **Results:** In lesions with <50% of neointimal CSA stenosis, homogeneous neointima (68.2%) was predominant, followed by heterogeneous neointima (14.1%) and layered neointima (14.1%). In lesions with \geq 50% of neointimal CSA stenosis, layered neointima was most frequently observed (68.3%), followed by neoatherosclerotic neointima (25.2%). In subgroup analysis of lesions with \geq 50% of neointimal CSA stenosis, 89.5% of the lesions with a stent age <30 months were layered neointima, while 62.3% of the lesions with a stent age \geq 30 months were neoatherosclerotic neointima. **Conclusion:** This study suggests that the OCT-detected morphology of DES neointimal tissue was different according to the follow-up time course and degree of neointimal hyperplasia.

Key Words: Optical coherence tomography, stent, coronary artery disease

INTRODUCTION

Optical coherence tomography (OCT) is able to provide the characterization of neointimal tissue and differentiate the various types of neointimal tissue that exist inside coronary stents.^{1,2} In addition, OCT revealed that neoatherosclerosis was the common mechanism of very late drug-eluting stent (DES) failure.^{3,4} Using OCT, we previously reported that the morphologic characteristics of neointimal tissues of DES restenotic lesions were different from those of non-restenotic le-

© Copyright:

Yonsei University College of Medicine 2014

This is an Open Access article distributed under the terms of the Creative Commons Attribution Non-Commercial License (<http://creativecommons.org/licenses/by-nc/3.0>) which permits unrestricted non-commercial use, distribution, and reproduction in any medium, provided the original work is properly cited.

sions.⁵ However, detailed information about the character of neointimal tissues is still insufficient because previous OCT studies were performed with relatively small study population.^{4,7} In the present study, therefore, we investigated the morphological features of neointimal tissue in a larger study population that had both a wide range of restenotic lesions and extended follow-up periods after DES implantation.

MATERIALS AND METHODS

Study design

A total of 1289 DESs were evaluated by follow-up OCT between September 2007 to July 2012. After the maximal percentage of cross-sectional area (CSA) stenosis was determined by OCT, five consecutive images of cross-sections at 1 mm intervals were identified. Among 1289 DESs, 725 DESs had ≤ 100 μm of mean neointimal thickness; other 57 DESs were excluded for poor quality of OCT images, totally occluded in-stent restenosis, or stent thrombosis. Thus, 507 DESs (418 patients) with >100 μm mean neointimal thickness were finally enrolled from the OCT registry database of our institute. The reasons for follow-up angiography were: 1) evaluation for myocardial ischemia (72 patients); or 2) planned angiography for itself or other segments (346 patients). General inclusion and exclusion criteria of the follow-up OCT procedures have been previously reported.⁸

The selection of DES at the time of coronary intervention was at the physician's discretion. Patients were treated with 117 sirolimus-eluting stents (Cypher[®], Cordis, Miami Lakes, FL, USA), 102 paclitaxel-eluting stents (Taxus[®], Boston Scientific, Natick, MA, USA), 204 zotarolimus-eluting stents (Endeavor sprint[®] or Resolute[®], Medtronic, Santa Rosa, CA, USA), 67 everolimus-eluting stents (Xience[®], Abbott Vascular, Abott Park, IL, USA), and 17 biolimus-eluting stents (Nobori[®], Terumo Corporation, Tokyo, Japan).

Stent implantation was performed using conventional techniques. Unfractionated heparin was administered as an initial bolus of 100 IU/kg, with additional boluses administered during the procedure to achieve an activated clotting time of 250 to 300 seconds. Dual anti-platelet therapy (aspirin and clopidogrel) was recommended to all patients for at least 12 months. This study was approved by the Institutional Review Board of our institute, and written informed consent was obtained from each patient.

OCT procedure and analysis

OCT was performed with either the Model M2 imaging system or the C7-XR[™] imaging systems (LightLab Imaging, Inc., St. Jude Medical, St. Paul, MN, USA). In the Model M2, the occlusion catheter was positioned proximal to the stent and a 0.014-inch wire-type imaging catheter was positioned distal to the stent. During image acquisition, the occlusion balloon (Helios, Avantec Vascular Corp., Sunnyvale, CA, USA) was inflated to 0.4 to 0.6 atm; lactated Ringer's solution was infused at 0.5 to 1.0 mL/s. The imaging wire was pulled from distal to proximal with a motorized pull-back system at 1.0 mm/s.⁸ The frequency-domain OCT system (Model C7-XR[™]) was developed to generate frames at much higher rates, thus allowing faster pullback speeds. OCT images were generated at a rotational speed of 100 frames/s, while a catheter was pulled back at 20 mm/s. A non-occlusive contrast medium was continuously flushed through a guiding catheter at a rate of 4 to 5 mL/s for 3 to 4 seconds. With both systems, continuous images were acquired and stored digitally for subsequent analysis.

All OCT images were analyzed at a core laboratory (Cardiovascular Research Center, Seoul, Korea) by analysts who were blinded to patient and procedural information. Cross-sectional OCT images were analyzed at 1-mm intervals for quantitative measurements and qualitative analysis in five consecutive cross-sections with a maximal percentage of CSA stenosis of neointima: $(\text{neointimal CSA}/\text{stent CSA}) \times 100$. Stent and luminal CSA were measured, and neointimal CSA was calculated as the stent CSA minus the luminal CSA. The stented segments with the maximal percentage of neointimal CSA stenosis were then assessed qualitatively to characterize neointimal tissue as 1) homogeneous neointima, an uniform signal-rich band without focal variation or attenuation; 2) heterogeneous neointima, focally changing optical properties and various backscattering patterns; 3) layered neointima, layers with different optical properties, namely an adluminal high scattering layer and an abluminal low scattering layer; and 4) neoatherosclerotic neointima, lipid-laden neointima, thin-cap fibroatheroma-like neointima, or neointima with calcification (Fig. 1).^{1,7,9} Lipid-laden neointima was defined as a signal-poor region with diffuse borders, and neointima with calcification was defined as a well-delineated, signal-poor region with sharp borders.⁹ To distinguish layered neointima from lipid-laden neointima, we considered a signal-poor region that fully masked the stent struts behind the neointima to be a lipid-laden neointima. A thin-cap fibroatheroma-like neointima was defined as

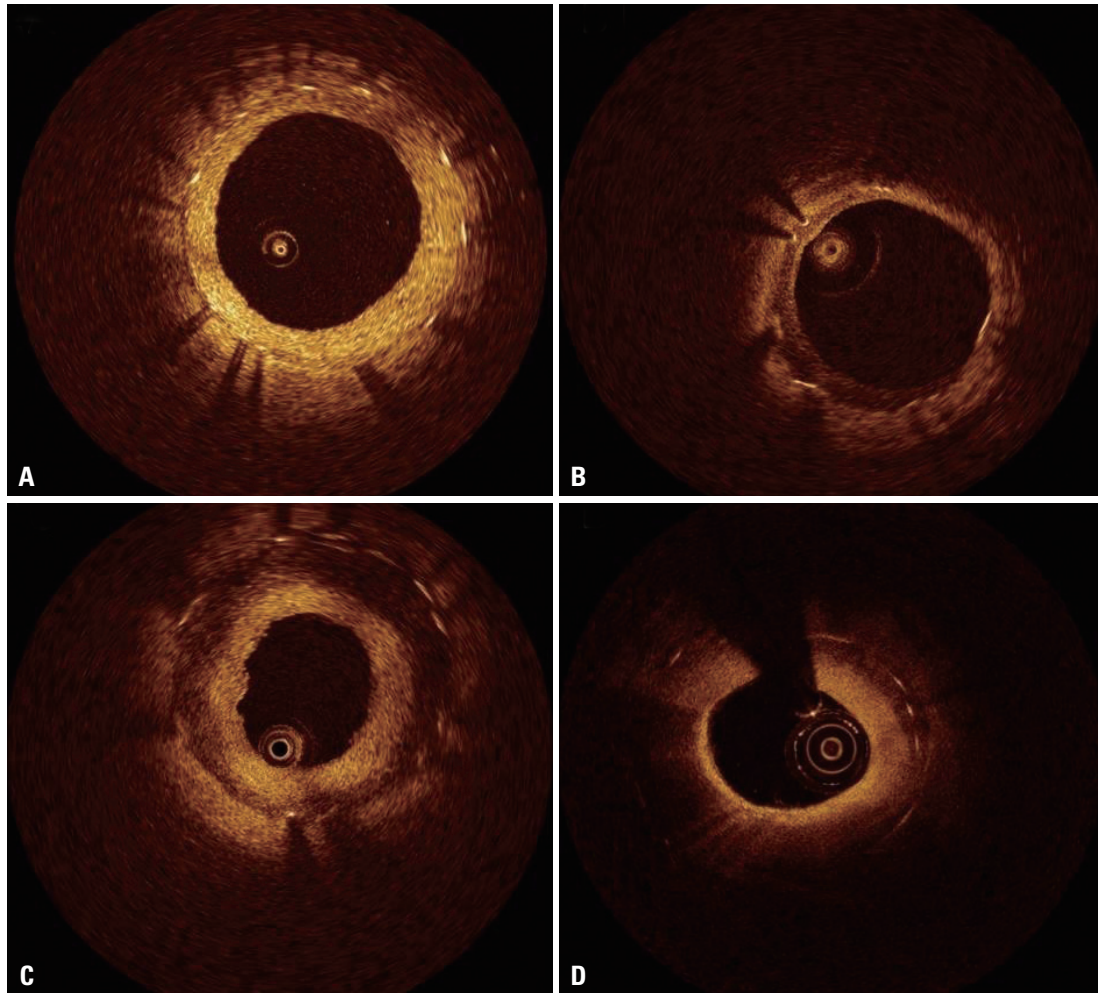


Fig. 1. Representative optical coherence tomographic images of neointimal tissue. (A) Homogeneous type. (B) Heterogeneous type. (C) Layered type. (D) Neoatherosclerotic type.

neointima with a fibrous cap thickness of $\leq 65 \mu\text{m}$ at the thinnest part and an angle of lipid-laden neointima $\geq 180^\circ$.^{7,9} Because the optimal cut-off time to predict neoatherosclerosis in DES-treated lesions was 30 months in our previous study,¹⁰ subgroup analysis of neointimal lesions with $\geq 50\%$ of CSA stenosis and a stent age of either ≥ 30 or < 30 months was performed. The inter- and intra-observer agreements for assessing neointimal tissue morphology in our laboratory were previously reported.⁵

Quantitative angiographic analysis

Quantitative coronary angiography analysis was performed using an offline computerized quantitative coronary angiographic system (CASS system, Pie Medical Imaging, Maastricht, the Netherlands). The minimal lumen diameter of treated coronary lesions and reference diameter at post-intervention and follow-up were measured in the view that was the narrowest and not foreshortened.

Statistical analysis

Statistical analysis was performed using PASW (version 18.0.0, SPSS Inc., Chicago, IL, USA). Data were expressed as number (%) or mean \pm standard deviation. Comparisons of categorical data were made using χ -square statistics or Fisher's exact test. Continuous variables were compared using Student's t-test or Mann-Whitney test. Multivariate logistic regression model was used to determine independent risk factors for neoatherosclerotic neointima. Variables with a p -value < 0.1 in univariate analysis were entered into the multivariate analysis. A p value < 0.05 was considered statistically significant.

RESULTS

There were no significant differences in the baseline clinical characteristics between the patients with $\geq 50\%$ and $< 50\%$

neointimal CSA stenosis (Table 1). Coronary angiographic findings are presented in Table 2. In lesions with $\geq 50\%$ of neointimal CSA stenosis, the intervention of the left circumflex artery and use of new-generation DESs, such as zotarolimus- or everolimus-eluting stent, were less frequently observed. Furthermore, in this group, the stent diameter was larger and the stent length was longer. OCT findings between the two groups are shown in Table 2. Time interval after index procedure was longer in lesions with $\geq 50\%$ of neointimal CSA stenosis. The morphologic features of the neointimal tissue according to the percentage of neointimal CSA stenosis (Fig. 2A) and time intervals of OCT after index procedure (Fig. 2B) are presented in Table 2. In lesions with $< 50\%$ of neointimal CSA stenosis, homogeneous neointima (68.2%) was the predominant morphology, followed by heterogeneous neointima (14.1%), and layered neointima (14.1%). In lesions with $\geq 50\%$ of neointimal CSA stenosis, layered neointima was the most frequently observed morphology (68.3%), followed by neoatherosclerotic neointima (25.2%). In a subgroup analysis of lesions with $> 50\%$ of neointimal CSA stenosis, the predominant morphology of the neointimal tissue was different according to the stent age. In lesions with a stent age < 30 months, layered neointima morphology (89.5%) was most frequently observed, while neoatherosclerotic neointima (62.3%) morphology was predominant in lesions with a stent age ≥ 30 months (Table 2, Fig. 3). While layered neointima was most frequently detected (70.4%) in patients with stable angina, neoatherosclerotic neointima was most common (71.4%) in patients with acute coronary syndrome (Table 3). The frequency of neoatherosclerotic neointima was higher in first-generation DES than in new-generation DES (20.5% vs. 1.0%, $p < 0.001$) (Table 4). Also, the frequency of statin usage was lower in lesions with neoatherosclerotic neointima

than those without (75.0% vs. 93.5%, $p < 0.001$) (Table 5). However, multivariate analysis showed that stent age was an independent predictor for neoatherosclerotic neointima (odds ratio, 1.130; 95% confidence interval, 1.092–1.170; $p < 0.001$).

DISCUSSION

This OCT study demonstrates that the morphological pattern of neointimal tissue after DES implantation depends both on the burden of neointimal hyperplasia and stent age. Homogeneous neointima was the most common morphology type in lesions with $< 50\%$ of neointimal CSA stenosis. In contrast, in lesions with $\geq 50\%$ of neointimal CSA stenosis, layered and neoatherosclerotic neointima were frequently detected. While layered neointima was largely attributable to in-stent restenotic lesions in lesions with a stent age < 30 months, neoatherosclerotic neointima contributed to neointimal growth in DESs ≥ 30 months after implantation. Layered neointima was the dominant morphology type in patients with stable angina, whereas neoatherosclerotic neointima was in patients with acute coronary syndrome.

The early vascular reaction after bare metal stent implantation is thrombus formation and acute inflammation around the strut, followed by neointimal growth.¹¹ In the early phase after stenting, fibrin, platelet, and inflammatory cells are nearly always observed in association with stent struts. They gradually disappear, as spindle-shaped mesenchymal cells (α -actin-positive smooth muscle cells) form a neointima within the proteoglycan matrix associated with the stent struts.¹¹ Although it is known that in-stent restenosis arises from the overwhelming growth of neointima, few pathologic studies have reported the detailed components of re-

Table 1. Baseline Clinical Characteristics

	<50% CSA stenosis (n=288)	$\geq 50\%$ CSA stenosis (n=130)	<i>p</i> value
Age (yrs)	61.7 \pm 8.8	62.9 \pm 9.8	0.217
Male	191 (66.3)	93 (71.5)	0.290
Diabetes mellitus	90 (31.3)	49 (37.7)	0.196
Hypertension	168 (58.3)	81 (62.3)	0.443
Hypercholesterolemia	112 (38.9)	60 (46.2)	0.162
Current smoker	51 (17.7)	32 (24.6)	0.101
Clinical diagnosis			0.677
Stable angina	216 (75.0)	95 (73.1)	
Acute coronary syndrome	72 (25.0)	35 (26.9)	

CSA, cross-sectional area.

Data are presented as mean \pm SD or n (%).

Table 2. Coronary Angiographic and Optical Coherence Tomographic Findings

Coronary angiography	<50% CSA stenosis (n=368)	≥50% CSA stenosis (n=139)	<i>p</i> value
Target lesions			0.004
Left anterior descending artery	183 (49.7)	85 (61.2)	
Left circumflex artery	77 (20.9)	12 (8.6)	
Right coronary artery	108 (29.3)	42 (30.2)	
Type of drug-eluting stent			0.006
Sirolimus-eluting stent	83 (22.6)	34 (24.5)	
Paclitaxel-eluting stent	63 (17.1)	39 (28.1)	
Zotarolimus-eluting stent	155 (42.1)	49 (35.3)	
Everolimus-eluting stent	57 (15.5)	10 (7.2)	
Biolimus-eluting stent	10 (2.7)	7 (5.0)	
Mean stent diameter (mm)	3.0±0.3	3.1±0.3	0.013
Mean stent length (mm)	27.9±13.3	31.8±16.8	0.035
Post-intervention			
Reference vessel diameter (mm)	2.9±0.4	2.9±0.5	0.960
Minimal lumen diameter (mm)	2.7±0.4	2.7±0.5	0.589
Follow-up			
Reference vessel diameter (mm)	2.8±0.4	2.7±0.5	0.409
Minimal lumen diameter (mm)	2.1±0.5	1.3±0.6	<0.001
Optical coherence tomography	<50% CSA stenosis	≥50% CSA stenosis	<i>p</i> value
Overall, n	368	139	
Time interval after index procedure (months)	14.0±11.9	28.1±23.2	<0.001
Mean neointimal thickness (μm)	245.5±89.4	617.1±188.5	<0.001
Mean lumen CSA (mm ²)	5.0±1.6	2.6±1.1	<0.001
Mean stent CSA (mm ²)	7.0±2.0	7.3±2.1	0.175
Mean neointimal CSA (mm ²)	2.1±1.0	4.7±1.6	<0.001
Percent neointimal CSA stenosis (%)	29.5±9.6	65.0±10.4	<0.001
Neointimal type			<0.001
Homogeneous	251 (68.2)	2 (1.4)	
Heterogeneous	52 (14.1)	7 (5.0)	
Layered	52 (14.1)	95 (68.3)	
Neoatheroma	13 (3.5)	35 (25.2)	
Stent age <30 months, n	332	86	
Time interval after index procedure (months)	10.7±6.1	12.2±5.5	0.001
Mean neointimal thickness (μm)	244.1±88.3	623.2±179.4	<0.001
Mean lumen CSA (mm ²)	5.0±1.6	2.7±1.1	<0.001
Mean stent CSA (mm ²)	7.1±2.0	7.7±2.0	0.014
Mean neointimal CSA (mm ²)	2.1±1.0	4.9±1.5	<0.001
Percent neointimal CSA stenosis (%)	29.2±9.4	64.2±10.1	<0.001
Neointimal type			<0.001
Homogeneous	230 (69.3)	1 (1.2)	
Heterogeneous	50 (15.1)	6 (7.0)	
Layered	48 (14.5)	77 (89.5)	
Neoatheroma	4 (1.2)	2 (2.3)	
Stent age ≥30 months, n	36	53	
Time interval after index procedure (months)	43.9±10.3	53.9±17.0	0.007
Mean neointimal thickness (μm)	259.0±98.7	607.1±203.8	<0.001
Mean lumen CSA (mm ²)	4.4±1.7	2.3±1.0	<0.001
Mean stent CSA (mm ²)	6.5±1.9	6.7±2.2	0.581
Mean neointimal CSA (mm ²)	2.0±0.8	4.5±1.7	<0.001
Percent neointimal CSA stenosis (%)	32.8±10.8	66.3±10.7	<0.001

Table 2. Continued

Optical coherence tomography	<50% CSA stenosis	≥50% CSA stenosis	<i>p</i> value
Neointimal type			<0.001
Homogeneous	21 (58.3)	1 (1.9)	
Heterogeneous	2 (5.6)	1 (1.9)	
Layered	4 (11.1)	18 (34.0)	
Neoatheroma	9 (25.0)	33 (62.3)	

CSA, cross-sectional area.

Data are presented as (%) or mean±SD.

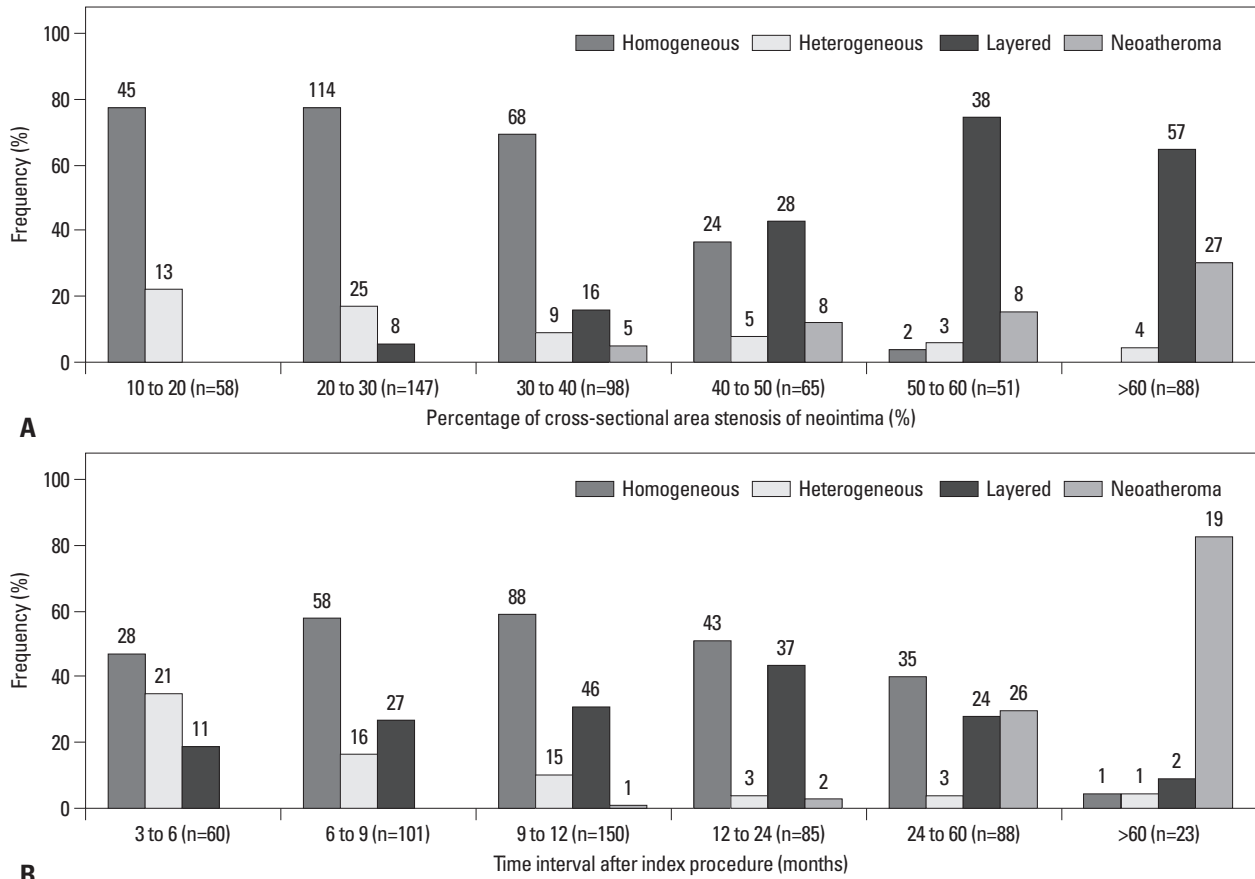


Fig. 2. Distribution of various neointimal tissues according to the percentage of neointimal cross-sectional area stenosis (A) and time interval of optical coherence tomography after index procedure (B).

stenotic tissue after DES implantation. Two previous reports that examined specimens from directional coronary atherectomy showed that restenotic tissue consisted of proteoglycan-rich smooth muscle cells and fibrinoid tissue, and this was considered as an evidence of incomplete neointimal healing after DES implantation.^{12,13}

Recent advances in intravascular OCT systems made it possible to visualize and characterize neointimal tissue. Comparing histological findings from autopsy reports to morphological patterns determined by OCT,¹⁴ homogeneous regions derived from OCT are shown to represent smooth muscle cells and indicated normal neointima. In this same study, fi-

brin accumulation, excessive inflammation, and in-stent neoatherosclerosis appeared as dark regions when assessed by OCT.¹⁴ Another pathologic study using specimens from directional coronary atherectomy showed that the layered pattern was composed of smooth muscle cells and myxomatous tissues which appeared as a hyperechoic inner layer and echolucent outer layer on OCT, respectively, while the heterogeneous pattern determined to be an organizing fibrin thrombus appeared as patchy and echolucent regions throughout the layer on OCT.¹⁵

Several *in vivo* OCT studies have revealed that various types of restenotic tissues can exist after DES implanta-

tion.¹⁻⁵ In 25 restenotic lesions with 12 months of median time after stent implantation, neointimal tissue structure was layered in 52%, homogeneous in 28%, and heterogeneous in 20%.¹ In another OCT study, homogeneous neointima

was observed in one third of a total 86 DES restenotic lesions.⁴ Among the non-homogeneous types of neointima, the thin cap fibroatheroma-like pattern neointima was observed more frequently in the early (<1 year) to the very

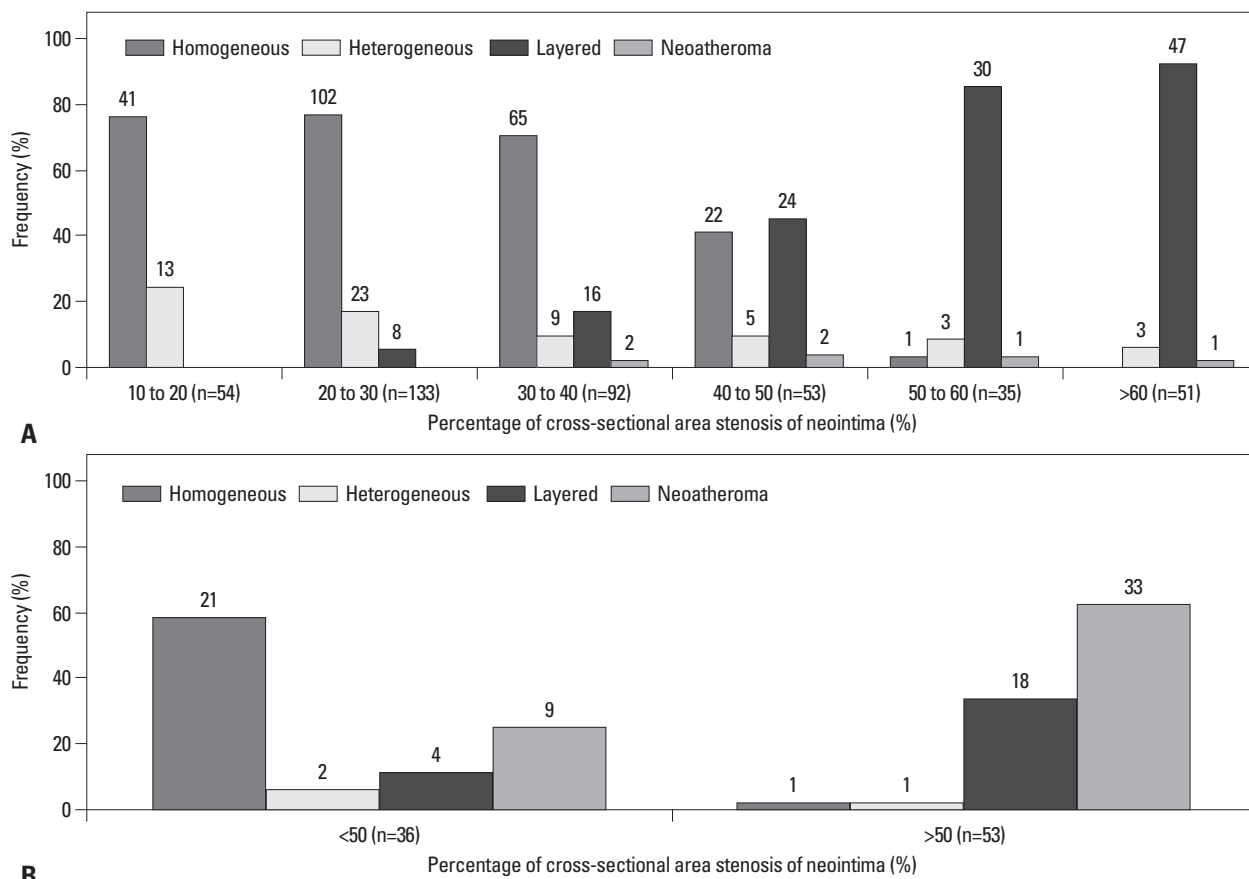


Fig. 3. Distribution of various neointimal tissues according to the percentage of neointimal cross-sectional area stenosis in lesions of stent age <30 months (A) and ≥30 months (B).

Table 3. Neointimal Types on Optical Coherence Tomography, Grouped by Clinical Presentations at Follow-Up

	Acute coronary syndrome (n=14)	Stable angina (n=54)	Asymptomatic (n=350)	<i>p</i> value
Neointimal type				<0.001
Homogeneous	0 (0.0)	2 (3.7)	189 (54.0)	
Heterogeneous	0 (0.0)	3 (5.6)	52 (14.9)	
Layered	4 (28.6)	38 (70.4)	91 (26.0)	
Neoatheroma	10 (71.4)	11 (20.4)	18 (5.1)	

Data are presented as n (%).

Table 4. Neointimal Types on Optical Coherence Tomography, Grouped by Drug-Eluting Stent

	First-generation drug-eluting stent (n=219)	New-generation drug-eluting stent (n=288)	<i>p</i> value
Neointimal type			<0.001
Homogeneous	91 (41.6)	162 (56.3)	
Heterogeneous	26 (11.9)	33 (11.5)	
Layered	57 (26.0)	90 (31.3)	
Neoatheroma	45 (20.5)	3 (1.0)	

Data are presented as n (%).

Table 5. Medications at Follow-Up, Grouped by Neoatherosclerosis on Optical Coherence Tomography

	Presence of neoatherosclerosis (n=48)	Absence of neoatherosclerosis (n=459)	<i>p</i> value
β-blocker	36 (75.0)	366 (79.7)	0.441
Angiotensin-converting enzyme inhibitor	15 (31.3)	156 (34.0)	0.703
Statin	36 (75.0)	429 (93.5)	<0.001

Data are presented as n (%).

late phase (>3 years). Although the particular classification of the neointimal tissues differs slightly from report to report, the OCT-based general observation that the homogeneous pattern was observed less frequently in in-stent restenotic lesions was a consistent finding.

Previously, we reported that the heterogeneous or layered neointima were observed more commonly in restenotic lesions than in non-restenotic lesions after DES implantation (78.8% vs. 22.9%, $p < 0.001$).⁵ However, there is still insufficient data to explain the vascular reaction after DES implantation. In the previous studies, the number of DES in-stent restenotic lesions ($\geq 50\%$ of neointimal CSA stenosis) was small, and the data for the morphologic features of the neointimal tissue in lesions $< 50\%$ of neointimal CSA stenosis were scarce.^{1,3-5} The present study was conducted with significantly larger population, and we found that the homogeneous neointima was the predominant morphologic type in lesions under 50% of neointimal CSA stenosis. This finding suggests that normal neointima was most common even in DES-treated lesions that did not show significant luminal narrowing. Although the layered and neoatherosclerotic patterns were mostly composed of in-stent restenotic tissues, the stent age affected the development of different patterns of in-stent restenosis. The layered pattern was the most common type observed in in-stent restenotic lesions with a stent age < 30 months, while the neoatherosclerotic pattern was more commonly observed in in-stent restenotic lesions with a stent age ≥ 30 months. This morphological difference suggests the patho-physiological mechanism causing DES restenosis changes with time, with neoatherosclerosis contributing to the late-phase narrowing of DES. These findings are consistent with those of previous OCT studies.^{3,4} Although the previous study evaluated neoatherosclerosis in lesions with $> 100 \mu\text{m}$ of mean neointimal thickness, various patterns of neointima were not addressed.¹⁶ Therefore, the present study could reflect the entire process of neointimal hyperplasia beyond neoatherosclerosis, with relatively large study population.

This study was limited by the possibility that selection bias could not be completely excluded. The quantitative and

qualitative assessment of OCT in entire stent was not performed. Volumetric evaluation of quantitative OCT findings was also not done. Comparison between DES and bare metal stent was not possible. Differences of target lesions between two groups might be coincidence. Furthermore, the characteristics of neointimal tissues have not yet been validated in histopathology studies.

In conclusion, the morphological features in DES-treated lesions assessed by OCT varied with the degree of neointimal burden as well as the stent age.

ACKNOWLEDGEMENTS

This study was supported by a grant from the Korea Healthcare Technology R&D Project, Ministry for Health, Welfare & Family Affairs, Republic of Korea (No. A085012 and A102064), a grant from the Korea Health 21 R&D Project, Ministry of Health & Welfare, Republic of Korea (No. A085136), and the Cardiovascular Research Center, Seoul, Korea.

REFERENCES

- Gonzalo N, Serruys PW, Okamura T, van Beusekom HM, Garcia-Garcia HM, van Soest G, et al. Optical coherence tomography patterns of stent restenosis. *Am Heart J* 2009;158:284-93.
- Lee SY, Hong MK. Stent evaluation with optical coherence tomography. *Yonsei Med J* 2013;54:1075-83.
- Kang SJ, Mintz GS, Akasaka T, Park DW, Lee JY, Kim WJ, et al. Optical coherence tomographic analysis of in-stent neoatherosclerosis after drug-eluting stent implantation. *Circulation* 2011;123:2954-63.
- Habara M, Terashima M, Nasu K, Kaneda H, Yokota D, Ito T, et al. Morphological differences of tissue characteristics between early, late, and very late restenosis lesions after first generation drug-eluting stent implantation: an optical coherence tomography study. *Eur Heart J Cardiovasc Imaging* 2013;14:276-84.
- Lee SJ, Kim BK, Kim JS, Ko YG, Choi D, Jang Y, et al. Evaluation of neointimal morphology of lesions with or without in-stent restenosis: an optical coherence tomography study. *Clin Cardiol* 2011;34:633-9.
- Yonetsu T, Kim JS, Kato K, Kim SJ, Xing L, Yeh RW, et al. Com-

- parison of incidence and time course of neoatherosclerosis between bare metal stents and drug-eluting stents using optical coherence tomography. *Am J Cardiol* 2012;110:933-9.
7. Takano M, Yamamoto M, Inami S, Murakami D, Ohba T, Seino Y, et al. Appearance of lipid-laden intima and neovascularization after implantation of bare-metal stents extended late-phase observation by intracoronary optical coherence tomography. *J Am Coll Cardiol* 2009;55:26-32.
 8. Kim U, Kim JS, Kim JS, Lee JM, Son JW, Kim J, et al. The initial extent of malapposition in ST-elevation myocardial infarction treated with drug-eluting stent: the usefulness of optical coherence tomography. *Yonsei Med J* 2010;51:332-8.
 9. Prati F, Regar E, Mintz GS, Arbustini E, Di Mario C, Jang IK, et al. Expert review document on methodology, terminology, and clinical applications of optical coherence tomography: physical principles, methodology of image acquisition, and clinical application for assessment of coronary arteries and atherosclerosis. *Eur Heart J* 2010;31:401-15.
 10. Lee SY, Shin DH, Mintz GS, Kim JS, Kim BK, Ko YG, et al. Optical coherence tomography-based evaluation of in-stent neoatherosclerosis in lesions with more than 50% neointimal cross-sectional area stenosis. *EuroIntervention* 2013;9:945-51.
 11. Farb A, Sangiorgi G, Carter AJ, Walley VM, Edwards WD, Schwartz RS, et al. Pathology of acute and chronic coronary stenting in humans. *Circulation* 1999;99:44-52.
 12. van Beusekom HM, Saia F, Zindler JD, Lemos PA, Swager-Ten Hoor SL, van Leeuwen MA, et al. Drug-eluting stents show delayed healing: paclitaxel more pronounced than sirolimus. *Eur Heart J* 2007;28:974-9.
 13. Chieffo A, Foglieni C, Nodari RL, Briguori C, Sangiorgi G, Latib A, et al. Histopathology of clinical coronary restenosis in drug-eluting versus bare metal stents. *Am J Cardiol* 2009;104:1660-7.
 14. Nakano M, Vorpahl M, Otsuka F, Taniwaki M, Yazdani SK, Finn AV, et al. Ex vivo assessment of vascular response to coronary stents by optical frequency domain imaging. *JACC Cardiovasc Imaging* 2012;5:71-82.
 15. Nagai H, Ishibashi-Ueda H, Fujii K. Histology of highly echolucent regions in optical coherence tomography images from two patients with sirolimus-eluting stent restenosis. *Catheter Cardiovasc Interv* 2010;75:961-3.
 16. Yonetsu T, Kato K, Kim SJ, Xing L, Jia H, McNulty I, et al. Predictors for neoatherosclerosis: a retrospective observational study from the optical coherence tomography registry. *Circ Cardiovasc Imaging* 2012;5:660-6.